DEUTSCHES ELEKTRONEN-SYNCHROTRON DESY

DESY SR-76/01
January 1976

Competition between Electronic Energy Transfer and Relaxation in Xe Doped Ar and Ne Matrices Studied by Photoelectron Spectroscopy

by

N. Schwentner
Christian Albrechts Universität, 23 Kiel

E. E. Koch
Deutsches Elektronen-Synchrotron DESY, Hamburg

2 HAMBURG 52 · NOTKESTIEG 1

To be sure that your preprints are promptly included in the
HIGH ENERGY PHYSICS INDEX ,
send them to the following address (if possible by air mail) :

DESY
Bibliothek
2 Hamburg 52
Notkestieg 1
Germany

Competition between Electronic Energy Transfer and Relaxation in Xe doped Ar and Ne Matrices Studied by Photoelectron Spectroscopy[≠]

N. Schwentner

Christian Albrechts Universität, 23 Kiel

and E.E. Koch

Deutsches Elektronen-Synchrotron DESY, 2 Hamburg 52

Thin films of solid Ar and Ne doped with 1 % Xe were excited with photons in the energy range from 10 eV to 20 eV in order to measure the energy distribution of the emitted electrons. Binding energies of the host and guest levels are deduced. When host excitons are excited, strong emission of electrons is observed indicating an efficient transfer of the host exciton energy to the Xe guest atoms. The energy of the free excitons is transfered as can be deduced from the kinetic energy of the photoemitted electrons rather than the energy of the bound (self trapped) excitons which are observed in luminescence experiments. Furthermore there is a striking difference between the Ar and Ne matrix: In the Ne matrix a fast relaxation from the n=2 to the n=1 state was observed and only the energy of the n=1 exciton is transfered even when higher excitons are excited, in contrast to Ar, where the transfered energy is higher for excitation of the n=2 excitons than for n=1. From these observations time hierarchies for the competition between electronic energy transfer and relaxation are deduced.

≠ Work supported by Deutsche Forschungsgemeinschaft DFG and Bundesminsterium für Forschung und Technologie BMFT

1. Introduction

Excitation of insulators by light, X-rays, γ-particles, protons, electrons or α-particles leads to the emission of light which is characteristic for the sample but rather independent of the special source. The dissipation of the excitation energy up to the point of luminescence has attracted increasing attention which is indicated by the large amount of recent contributions dealing with problems of radiationless transitions.[1] In the present study photoelectron energy distribution measurements where the energy of the exciting light could be varied, have been used to investigate such decay processes.

During the last decade, the optical properties of fundamental insulators viz the rare gas solids[2], and their luminescence spectra[3-6] have been studied. The absorption spectra are dominated by exciton series which converge in a hydrogenic fashion to the band gap. The energies of the luminescence bands are smaller than the lowest absorption line and the emission is attributed to trapped excitons i.e. the decay of vibrationally relaxed, electronically excited homonuclear rare gas diatomic molecules[7].≠ Besides theoretical interest, the efforts to develop more efficient VUV lasers stimulate the study of the involved decay channels, including a special radiationless transition involving the energy transfer of host excitation energy to guest atoms in doped rare gas solids.[9] From theoretical estimates[10,11] and from the results of recent photoelectron yield studies[12], it is expected that many relaxation processes are fast with time constants in the 10^{-11} sec to 10^{-13} sec range. By application of ultrashort light pulses from mode locked lasers, decay measurements in the picosecond time scale have been carried out[13]. Such light sources are not available for the high photon energies ($\hbar\omega > 8$ eV) which are required for the large band gaps of the rare gas solids. Thus one is restricted to less direct experiments.

≠ For the special case of solid Ne see Ref. 39

In recent luminescence experiments, efforts have been made to obtain more information about these states by the use of monochromatic radiation[5]. By these means, different states can be separately populated. However, the resulting light emission is mainly observed from the lowest states.

Thus new experiments are required in order to determine both the energies of the upper states and the time hierachy involved.

From the energy distribution curves (EDC) of photoelectrons, the structure of valence bands and the lowest conduction bands of all the rare gas solids has been deduced.[14] For highly excited electrons with kinetic energies exceeding the band gap E_G (excitation energy $\geq 2\ E_G$) the scattering length for electron -electron inelastic scattering falls from $\approx$ 1000 Å to below 10 Å[15]; i.e. a time constant for this process shorter than $\approx 10^{-15}$ sec. The kinetic energy of low energy electrons in the conduction band is dissipated only by interaction with the lattice (phonons, defects) because inelastic electron-electron scattering is forbidden by the band gap[15,16].

In this paper we are mainly concerned with relaxation processes in the excitonic region below the bottom of the conduction band. The exciton series observed in optical spectra of pure and doped rare gas solids can be satisfactorily interpreted in terms of Wannier series converging to the bottom of the conduction band for the members $n \geq 2$.[3] The lowest exciton (n=1) is of the intermediate type (between Wannier and Frenkel) but can be described by a n=1 Wannier state subjected to a large central cell correction[3]. For Ar, Kr and Xe and the impurity states of these elements two series split by the spin orbit coupling in the np-valence shells are exhibited. They are denoted by n(j=3/2) and n'(j=1/2) (see Fig. 1). The n=1 and n=2 exciton states lie below the vacuum level and do not contribute to photoelectron

emission directly[2,17,18]. Recent photoelectron yield measurements of pure and doped Ar and Ne showed that these excitons decay and excite electrons above the vacuum level via energy transfer to guest atoms or to the gold substrate[12,36]. From the knowledge of the incident photon energy and the observed kinetic energies of the electrons in the EDC's the relaxation energy before energy transfer can be deduced. Thus we can compare the relaxation time to different states with the time constant for energy transfer. For example, when the n=2 exciton of the host is excited a competition between relaxation to the n=1 exciton, relaxation to the selftrapped exciton and energy transfer to guest atoms is expected. For Ar and Ne, theoretical calculations for both relaxation time constants are available[10,11] The difference in binding energies of n=1 and n=2 states in Ar as well as in Ne exceeds 1 eV and can be well resolved with the resolution of our electron analyzer of 0.2 eV. The impurity states of Xe lie high enough above the host valence band to be ionized even by the n=1 exciton of the host. The various possible processes are scetched in Fig. 1b.
After a short description of the experimental arrangement (section 2) EDC's for 1 % Xe in Ar and 1 % Xe in Ne matrix are presented for several photon energies (section 3). The energies involved are discussed in section 4 while the time hierachy is deduced in section 5.

11. Experimental procedure

The synchrotron radiation of the Deutsches Elektronen-Synchrotron DESY together with a normal incidence monochromator (resolution 2 Å) served as a light source for photon energies from 5 eV to 30 eV with a photon flux at the sample of typically 10^9 photons per second[20,21]. Attached to the UHV sample chamber (typical pressure 1×10^{-10} Torr) were (1) a bakeable liquid He cryostat (2) an electron energy analyzer (3) a turnable open photomultiplier to measure the sample reflectance and (4) an UHV gas handling system (Fig. 2).

The incident light beam hits the sample with an angle of incidence of 45^{o}, illuminating an area of 10 mm^2. A gold film served as a substrate which was isolated from the cryostat by a quartz disk. The photoelectrons were preaccelerated by the applied bias voltage V_p of 5 V. The electron energy analyzer is mounted normal to the sample surface and accepts electrons within a cone of 3^{o}. The electrons are selected according to their energy by a combination of a retarding grid and electrostatic lenses. Counting rates of 1000 counts/sec were typical. For more details see Ref. 21.

Photoelectron-emission measurements on rare gas solids are hampered by strong charging effects[15a,22]. Sample charging was minimized by the preparation of thin films with thicknesses of the order of 50 Å. The growth of the films was monitored during deposition of the gas by measuring continuously the oscillations in the reflectance in the transparent region of the material (Ar 1100 Å, Ne 800 Å). For the calculation of the film thickness, the formulae of Ref. 23 were applied to the solid rare gas Au sandwich with optical constants taken from the literature[24,25]. Further the illumination time was held to a minimum (1-5 minutes per spectrum) to avoid accumulation of charge. Consequently the statistics were not always as good as might be desired. In the spectra presented charging was less than 0.3 eV.

For the preparation of the films Matheson research grade gases with a purity of better than 99.997 for Xe, 99.9999 % Ar and 99.995 % for Ne were used. The given doping concentrations correspond to the ratio of the partial pressures of the constituents in the gas handling system

(total pressure 1000 Torr). The Xe/Ne mixtures were frozen at substrate-temperatures of 6 K, the Xe/Ar mixtures at 15 K. No attempts for annealing were made.

III. Results

3.1 Xe in Ar

In the right part of Fig. 3 EDC's of a 50 Å thick film of 1 % Xe in Ar are presented for several photon energies as a parameter. In order to show clearly the structure within each EDC the counting rates for each spectrum are arbitrarily normalized. For a quantitative comparison the total areas of the EDC's normalized to the same incident light intensity are given by the crosses in the left part of Fig. 3. They are compared with the yield curve of a 60 Å thick film of 1 % Xe in Ar as determined in Ref. 12. Here and in Fig. 4 a structureless background caused by hot electrons from the gold substrate was subtracted from the yield and EDC spectra. For $\hbar\omega$ = 16 and 19 eV (Fig. 3) this background was not subtracted in order to show its contribution to the EDC's.

From Fig. 3 the common features of the yield curve and the total areas of the EDC's of a strong enhancement in (1) the region of the n=1 and n=2 excitons and (2) in the region of interband transitions are immediately evident. However, quantitative agreement cannot be expected because of the different angle of incidence of the light. Furthermore, in the EDC's only electrons within a cone of 3° are accepted, whereas in the yield spectra all the emitted electrons are collected.

In the EDC's the zero kinetic energy corresponds to the vacuum level of the Xe/Ar-Au-sandwich. The vacuum level was determined from the low energy onset

of EDC's of the gold substrate, taken before depositing the rare gas. After preparation of the thin films this onset is the same for electrons excited in the sample ($\hbar\omega$ = 16 eV) as well as for hot electrons from the Au substrate ($\hbar\omega$ = 19 eV) indicating no change of the Au work function on evaporation.

In Fig. 3 and 4 the baselines of the spectra are shifted upwards according to the exciting photon energy. The kinetic energies E_{kin} of the maxima and onsets increase in proportion to the photon energy $\hbar\omega$ as is expected from the relation

$$E_{kin} = \hbar\omega - E_{Th} \qquad (1)$$

and demonstrated by the diagonal lines, Here E_{Th} (threshold energy) is the binding energy of the initial state measured relativ to the vacuum level E_V.

With photon energies from 11 eV up to 19 eV, the three different regions of excitation are covered:

1. At low photon energies ($\hbar\omega \leq$ 12 eV) the Ar host matrix is transparent. Only guest atoms are excited.
2. In the region of host exciton excitation (12 eV $\leq \hbar\omega \leq$ 14 eV) efficient energy transfer to the guest atoms takes place as will be discussed in section 5. For this region more EDC's with an expanded photon energy scale are shown in Fig. 4.
3. For photon energies above 14.2 eV the gap energy E_G^{Ar} of the Ar matrix, electrons from the guest atoms as well as from the valence band of the host are excited into the conduction bands of the host.

The strong increase of the counting rate and the change in shape for Xe in Ar relative to the gold substrate is demonstrated for n=1, $\hbar\omega$ = 12.25 eV in Fig. 5. Pure Ar of 45 Å thickness yields a comparitively small increase

in counting rate and an EDC peaking near zero kinetic energy, a spectrum rather similar to that of Au. For the spectra shown in Fig. 6, the energy of transmission of the electron energy analyzer was fixed to E_{kin} = 0.2±0.2 eV and the photon energy was scanned (constant final state spectra). The crosses represent the corresponding counting rates of the EDC's of the 1 % Xe/Ar matrix from Fig. 4 normalized to the incident light intensity. For the discussion it is important to keep the following observations in mind:

a) There is a definit increase in counting rate for the Xe/Ar sample at electron energies near the vacuum level both when the n=1 and the n=2 excitons are excited.
b) For thicker films of Xe/Ar (not shown), the counting rate in the excitonic region increases (see also Ref. 12).
c) The shape of EDC's for pure Ar is clearly different from curves of the doped samples.
d) The enhancement for pure Ar for a film of 45 Å thickness is smaller than for the doped sample and with increasing thickness (d = 135 Å), the counting rate in the excitonic region decreases, especially in the center of the n=1 exciton band and stays constant for the n=2 excitons (Fig. 6).

The binding energies of the initial states can be derived from the EDC at $\hbar\omega$ = 19 eV (Fig. 3). The variation of the photon energies (see diagonal lines) makes possible an increase in accuracy by averaging. Furthermore shifts due to possible strong structure in the final states are not observed.

At $\hbar\omega$ = 19 eV and $\hbar\omega$ = 16 eV most electrons stem from the Ar 3p valence bands. They produce the large peak in the left shadowed region (Fig. 3). From the kinetic energy of the high energy onset we obtain (equ. 1) a

binding energy for electrons at the top of the Ar 3p valence bands of E_{Th}^{Ar} = 13.9 eV. The shadowed region indicates the width of the Ar 3p valence bands, E_{VBW}^{Ar}, of 1.8 ± 0.2 eV. Due to the smaller ionization energy, the Xe, 5p guest levels are located within the Ar band gap. The maximum with the highest kinetic energy corresponds to the Xe 5p 3/2 level, the second to the Xe 5p 1/2 level. The centers of the peaks are connected with diagonal lines. Their separation gives a spin orbit splitting of the Xe 5p states in an Ar matrix of 1.3 ± 0.1 eV. The high energy onset of the Xe excitations (dashed line) shows that the Xe 5p 3/2 level lies 3.5 eV above the top of the Ar valence bands: $E_{Th}^{Ar} - E_{Th}^{Xe/Ar}$ = 3.5 eV, yielding a binding energy of the Xe 5p 3/2 level, $E_{Th}^{Xe/Ar}$, of 10.4 ± 0.2 eV. Together with the spectroscopically determined gap values[2,26] of E_G^{Ar} = 14.15 eV and $E_G^{Xe/Ar}$ = 10.54 eV we get for the electron affinity, V_o, a value of V_o = 0.14 ± 0.2 eV where

$$V_o = E_G - E_{Th} \qquad (2)$$

V_o is the difference between the bottom of the conduction band and the vacuum level. All these values are compiled in Table 1. As far as solid Ar is concerned they corroborate within the experimental limits the values reported earlier[14]. The width of the Xe 5p excitations may be partly due to the interaction of neighbouring guest atoms. A close proximity is likely at doping concentration of 1 %. We have investigated films with thicknesses up to several hundred Å. Aside from an increase in counting rates caused by stronger absorption in the film, the main features remain and thus the given quantities are bulk properties. Charging in thicker films because of the greater separation of the positive charges from the gold substrate is stronger. The whole EDC shifts to lower kinetic energies but it can still be observed because of the pre-accelerating voltage V_p. Additionally, the EDC's are broadened by the not uniform distribution of the charges across the film. From the ob-

served time and thickness dependence, we conclude that charging was smaller than 0.2 eV for the spectra below $\hbar\omega$ = 13 eV, which were measured first and smaller than 0.3 eV for the others.

The weak maximum with the long tail near zero kinetic energy in the spectrum for $\hbar\omega$ = 19 eV (Fig. 3) is caused by hot electrons from the gold substrate. From its area we get a rough estimate for the photoemission efficiency of our films. From the absorption coefficient[2], μ, für Ar of $\approx 6 \times 10^5$ cm^{-1}, it follows that 75 % of the incident light reaches the gold substrate. The absorption of Xe atoms is negligible because of the small concentration. Provided no electrons escaping from the gold are lost in the Ar film, we calculate from the ratio of the contributions from Au and from Ar an efficiency of Ar which is 7.5 times that of Au. This assumption is reasonable according to Ref. 12. With the efficiency of Au of 5 % to 9 %[27], we get for Ar an efficiency of 0.5 electrons emitted per photon absorbed. This value is close to the experimental result of Ref. 17 but it has to be kept in mind that we have neglected any dependence on the angle of emission.

3.2 Xe in Ne

EDC's of 1 % Xe in Ne for excitation energies below the host absorption edge ($\hbar\omega$ = 16 eV), in the n=1 exciton band ($\hbar\omega$ = 17.5 eV) and in the n=2 exciton band ($\hbar\omega$ = 20.4 eV) are presented in Fig. 7. A structureless background due to hot electrons from the gold substrate was subtracted. The counting rates for the spectra can not be compared, since they are arbitrarily normalized. Again the baselines of the spectra are shifted according to the photon energy and the solid diagonal line represents the expected increase of electron kinetic energy with photon energy (eq. 1). Obviously, when n=2 excitons of the Ne host are excited, eq. 1 does not hold and a considerable amount of energy, mor than 3 eV, is missing. This striking observation, which differs from

what was observed for Xe in Ar is discussed in section 5 in view of the relation between energy transfer and relaxation.

The two maxima observed represent the Xe 5p 3/2 and Xe 5p 1/2 states in the band gap of the Ne matrix. Their separation gives a spin orbit splitting of 1.25 ± 0.1 eV for the Xe atoms in a Ne matrix. At $\hbar\omega$ = 16 eV, only the Xe guest atoms can be excited and we do not expect relaxation processes to affect the kinetic energy of the electrons. The energy of the high energy onset (4.8 eV) of the 3/2 level leads to a threshold energy, $E_{Th}^{Xe/Ne}$, of 11.2 eV. In the doped sample, the same EDC of the 2p valence bands of Ne as in Ref. 14 were observed. Thus with the value of V_o = 1.4 eV[14] a band gap, $E_G^{Xe/Ne}$, for Xe in Ne of 12.6 ± 0.2 eV is determined in agreement with Ref. 31 (see Table 1).

IV. Discussion of the impurity states

From our experiments the binding energies and the spin orbit splitting of the Xe 5p states in solid Ar and Ne matrices were determined (Table 1). The spin orbit splitting of 1.3 eV is, within the experimental accuracy, independent of the host matrix and very close to the value in the gas phase. It also agrees with the calculated spin orbit splitting for pure solid Xe at the center of the Brillouin Zone[28]. The spin orbit splitting in EDC's of pure solid Xe is masked by the overlap of the upper and lower valence bands brought about by their $\underline{k}$-dependence. Further in optical spectra of pure Xe a well developed exciton series for the Xe 5p 1/2 excitation is missing and therefore the value of 0.9 eV resulting from an extrapolation of the exciton series[2] is uncertain. The separation of 1.17 eV observed in pure solid Xe for the n(3/2)=1 exciton[2] may be closer to the true value for the splitting. In view of these facts the value of 1.3 eV for the spin orbit splitting of pure Xe is plausible.

From the binding energies $E_{Th}^{Xe/Ne}$ and $E_{Th}^{Xe/Ar}$ together with the excitation energies of the n=1 excitons, the position of the later below the vacuum level can be calculated. Using the electron affinity, V_o, the exciton binding energy, B (the difference of excitation energy and bottom of the conduction band) is determined. Both the spin-orbit splitting and the binding energy B contradict the identification of the exciton series of Xe in Ne given by Baldini[30]. The results here are in excellent agreement, however, with the new values and assignments of Pudewill et al.[31]. For Xe in Ar our analysis is in accordance with Baldini[26]. The present investigation of the EDC's confirms the interpretation of the optical spectra in terms of Wannier series. The discrepancy of our B value with that of Gedanken et al.[32] has consequences for the central cell correction of the n=1 excitons. According to the calculation of Hermanson[33] the central cell correction for a specific guest atom in different matrices depends only on the binding energy B. With the new B value for Xe in Ne, the linear dependence of B stated by Gedanken et al. does not hold as is discussed in Ref. 31.

V. Energy transfer and relaxation

In Ar and Ne matrices an efficient transfer of the host exciton energy to the Xe guest atoms is observed. The main difference, documented in Fig. 4 and Fig. 7, is the increase of the energy of the emitted electrons proportional to the excitation energy in Ar, whereas it stays constant for the n=1 and n=2 excitons in Ne. Furthermore the efficiency of the energy transfer process in Xe/Ar is strongly dependent on the excitation energy, i.e. whether interband or exciton states are excited in the primary absorption process. In the following these observations will be discussed, see also Fig. 1b.

5.1 Xe in Ar

5.1.1 Interband transitions of the Ar host

The photon energy $\hbar\omega$ = 19 eV is sufficient to excite electrons from the whole Ar valence bands into the Ar conduction bands (Fig. 3). Previous yield measurements of pure Ar[17] showed an efficiency of 0.6 electrons/photon absorbed. Yield spectra of thin films of Xe doped Ar[12] indicated a comparable efficiency, but it could not be decided whether the electrons were emitted by the host or the guest atoms. The different origins of the electrons are clearly separated in the EDC's in Fig. 3. The contribution of electrons from the Ar 3p valence bands is 80 times that of Xe 5p states at 16 eV and 40 times at 19 eV. This result, namely that the electrons are emitted with a probability roughly according to the atomic concentrations leads to the conclusion that they stem from distinct photon absorption processes at Ar or Xe atoms respectively. The deviations from the given mixing concentrations may be due to different absorption coefficients of guest and host atoms and to an enrichment of Xe in the Ar matrix during solidification. An enrichment factor of 2 (or of 3 when taking into account the energy dependence of the Ar absorption constant), is in agreement with the observation of Baldini.[30] In any case we can give an upper limit of 0.01 for the efficiency of the energy transfer process to Xe atoms both for excitation energies of 16 eV and 19 eV. We conclude that for the Ar interband transitions no energy transfer or at most with an efficiency below 0.01 takes place in photoemission.

This observation does not exclude the possibility that in luminescence experiments energy transfer will be seen when electrons are excited into the conduction band. As stated beforeluminescence is a much slower process than photoelectron emission, since for the light emission the hole has to

capture an electron again. Before light is emitted the captured electron may relax from the conduction band to exciton states (see calculation of Ref. 11). Finally energy transfer may take place from this host exciton states to the Xe guest, a process discussed in 5.1.2. Alternatively the hole in the Ar valence band may be filled by an electron from the Xe guest atoms instead of a free electron. The resulting hole at the Xe guest atom may subsequently capture an electron leading to radiative decay. The observed photon energy will be equal to that from the energy transfer processes.

5.1.2 Ar excitonic region

An increase of electron emission from the Xe guest atoms of two orders of magnitude is observed in the Ar host exciton regime. According to the Ar absorption constant[25] in the n=1 exciton 80 % of the light will excite Ar excitons and only 0.003 % should ionize the Xe guest atoms directly for the film thickness of 50 Å. The n=1 and n=2 excitons lie below the Ar vacuum level. They can contribute to photoemission only by secondary processes. (This is evident from an extrapolation of the kinetic energy of the Ar valence band excitations in Fig. 3). Now let us consider the various possible processes. Energy transfer to the gold substrate yields only a small contribution. As observed for pure Ar[19] and studied for pure Xe[34] it has a much lower efficiency and a different dependence on thickness (see Fig. 5, 6 and Ref. 19) than observed for Xe in Ar. Further the shape of the EDC from pure Ar at $\hbar\omega$ = 12.25 eV is similar to that of Au and does not correspond to that of Xe in Ar (Fig. 5). We conclude that almost all of the emitted electrons in the excitonic region are produced by an energy transfer process to the Xe atoms. There the yield almost reaches the same value as in the maximum of host emission in the interband regime at $\hbar\omega \approx 15$ eV.

In Ref. 12 the dependence of the total yield on film thickness and Xe concentration was studied and interpreted in terms of a diffusion model. The EDC's give more detailed insight in the transfer process.

Energy transfer from the n=1 excitons:

For photon energies of 11 eV and 11.5 eV the Ar matrix is transparent and the Xe atoms are excited directly. No deviations from the straight connections of onsets and peak positions in the EDC's from direct excitations at $\hbar\omega$ = 11 and 11.5 eV with those at $\hbar\omega$ = 16 and 19 eV is observed for $\hbar\omega$ = 12.07 and 12.25 eV. Thus we have to exclude dissipation of energy by relaxation prior to energy transfer from the n=1 and n'=1 exciton states to the Xe guest, at least within the experimental limit of 0.2 eV.

On the basis of luminescence spectra resonant energy transfer from the self-trapped matrix excitons to the guest atoms was assumed in Ref. 35. Generally in luminescence experiments of pure solid Ar emission from the selftrapped excitons is observed (Fig. 8). The strongest emission band found in all investigations is centered at 9.8 eV. Its intensity falls below 10 % within ±0.5 eV (Fig. 8). Therefore even the high energy part of this molecular emission band is not sufficient to ionize the Xe atoms with the observed efficiency. (Note that the ionization energy for Xe atoms in an Ar matrix is 10.4 eV) Furthermore the energy of the selftrapped excitons is more than 2 eV to low to ionize both spin orbit split levels (Fig. 8). Therefore we have to reject the resonant energy transfer process from selftrapped host excitons, which was proposed in Ref. 4 as the major energy transfer mechanism. Rather the energy of the free excitons is transfered to Xe guest atoms. In Ref. 5

and in Ref. 6 weak luminescence bands at higher energies have been detected under certain conditions (Fig. 8). It is still an open question if they belong partly to emission from free excitons. Again the intensity and the energies are too small to explain the EDC.

The difference in the shape of the EDC for excitation of the n(3/2)=1 at 12.07 eV and of the n'(1/2)=1 at 12.25 eV (Fig. 4) can be attributed to larger values of the transfered energy, which allows also ionization of the lower Xe 5p 1/2 level. This difference demonstrates that relaxation of the n'=1→n=1 needs more time than energy tranfer. Summarizing the observations for the n=1 and n'=1 exciton we obtain for 1 % Xe in Ar:

1) Energy transfer (time constant τ_T) is faster than radiative decay (τ_D):

$$\tau_T < \tau_D.$$

2) τ_T is smaller than the relaxation time constant τ_R^t to bound states (trapped exciton): $\tau_T < \tau_P^t$.

3) τ_T is smaller than the relaxation time constant $\tau_R(n=1 \rightarrow n'=1)$ for relaxation of n'=1 to n=1 exciton: $\tau_T \ll \tau_R(n=1 \rightarrow n'=1)$.

Using the oscillator strength of the n=1 exciton of Ar[25] a time constant of $\tau_D \approx 10^{-9}$ sec is estimated for the radiative decay of these excitons. From the dominant contribution of the self trapped excitons to luminescence of pure Ar a ratio of $\frac{\tau_R^t}{\tau_D} \lesssim \frac{1}{100}$ was estimated by Gedanken et al.[35] resulting in an upper limit for τ_R^t of 10^{-11} sec. This agrees with a calculation of Martin[10] which predicts a dissipation of energy of 0.5 to 1 eV within a time of 10^{-12} sec by self trapping of the exciton in solid Ar. According

to our EDC's, the relaxation energy before energy transfer is smaller than 0.2 eV leading to the following time hierarchy

$$\tau_D \gtrsim 10^{-9} > \tau_R^t \gtrsim 10^{-12} > \tau_T$$

and

$$\tau_R(n=1\rightarrow n'=1) > \tau_T \ .$$

Energy transfer from higher excitons n=2, n'=2.

The shape of the EDC's changes with photon energy (Fig. 4). At higher energies a third maximum, A, appears near the vacuum level. At lower photon energies this maximum partly overlaps with that of the Xe 5p 1/2 level. But at energies corresponding to the n=2 ($\hbar\omega$ = 13.58 eV) and n'=2 ($\hbar\omega$ = 13.79 eV) exciton states the maxima B and C are clearly separated from maximum A (Fig. 4). Thus the EDC can be separated into two parts: maxima B and C which are caused by electrons from an ionization process of the Xe 5p ($\frac{3}{2}$) and Xe 5p($\frac{1}{2}$) level, and maximum A at higher energies, which possibly contributes with a flat background to B and C.

First we conclude that the relaxations times $\tau_R(n=2\rightarrow n=1)$ and $\tau_R(n=2'\rightarrow n=1')$ for the processes n=2→n=1,1' and n=2'→n=1,1' are long compared to the processes leading to photoemission, because the maxima A, B and C do not correspond in their kinetic energies and shape to the EDC's at the excitation energies of the n=1 or n'=1 excitons. Next we attribute the maxima B and C to energy transfer of the free (i.e. not relaxed) n=2 (n'=2) excitons to the Xe guest atoms, because they are located at the diagonal lines (Fig. 4, eq. 1).

The origin of the maximum A and the background contribution to B and C causes some problems. Since it appears at photon energies below E_{Th}^{Ar} it must

originate from an energy transfer process. One possibility may be energy transfer to the gold substrate as was observed for pure Ar (Fig. 6). For a 135 Å thick film of pure Ar the intensity of slow electrons is reduced in the region of the n=1 exciton, as we would expect from the small penetration depth of the light, with the consequence that the excitons are excited in a greater distance from the substrate, leading to lower efficiency of energy transfer to the gold (see also Ref. 34). In the region of the n=2 and n'=2 excitons of pure Ar, because of the larger penetration of the light, photoemission stays constant according to the balance of increased absorption in the film and reduced efficiency of energy transfer to the substrate. However, for the origin of the peak A in the EDC's from Xe doped Ar we rule out the energy transfer to the Au substrate:

1) For a 45 Å thick film of pure Ar there is an increase in photoemission compared to pure gold, but the increase is a factor of three less than the contribution of maximum A for a 50 Å thick film of 1 % Xe in Ar (see Fig. 5,6).

2) In addition the ratio of maximum A to maximum B or C did not change markedly with film thickness. If maximum A would be produced by energy transfer to the substrate the ratio should be lowered for thicker films because the excitons are excited at a larger distance from the substrate and energy transfer to the Xe atoms (maximum B and C) should be favoured.

For these reasons energy transfer to the gold substrate can only be a process of minor significance in forming maximum A. We rather suggest, that maximum A is due to energy transfer from partly relaxed excitons. Since the major part

of peak A has kinetic energies lower than from the direct transfer from n=1 and n=2 states maximum A originates from energy transfer of bound exciton states.

We then would have to state that excitation of the n=1,1' excitons leads to a direct energy transfer prior to relaxation, whereas excitation of the n=2,2' excitons partly leads to direct energy transfer (peak B and C) and partly to energy transfer from a relaxed bound exciton state (peak A). This different behaviour of the n=1 and n=2 excitons can be attributed to a lower energy transfer rate or a faster trapping time τ_R^t of the n=2 excitons.

After relaxation by $\gtrsim$0.3 eV the energy above the trapping minimum is dissipated very fast, according to the calculation of Martin[10]. Because we observe in the EDC of the n=2 excitons also appreciable energy transfer of free excitons, the time constant for energy transfer, τ_T, may be only slightly larger than the trapping time τ_R^t. Radiative decay (τ_D) has only been detected from lower states than n=2. Thus the following time hierarchy is obtained:

$$\tau_D > \tau_R(n=2\rightarrow n=1) > \tau_T > \tau_R^t.$$

With our estimated τ_D and τ_R^t from the calculation of Martin we get upper and lower limits for $\tau_R(n=2\rightarrow n=1)$: 10^{-9} sec > $\tau_R(n=2\rightarrow n=1)$ > 10^{-12} sec. Webman et al.[11] deduced from a model calculation a relaxation time constant for an impurity state in solid Ar: $\tau_R(n=2\rightarrow n'=1) \gtrsim 10^{-11}$ sec, a result compatible with the limits obtained above. Taking these number leads to:

$$\tau_D \gtrsim 10^{-9} \text{ sec} > \tau_R(n=2\rightarrow n'=1) \gtrsim 10^{-11} \text{ sec} > \tau_T \simeq \tau_R^t \gtrsim 10^{-12} \text{ sec}$$

The consequences of the energy dependence of the energy transfer rate constant should be reconciled with the explanations in terms of an exciton

diffusion or Förster Dexter model or with an integration of both[12,34]. For this discussion the information from the present EDC measurements seems not to be sufficient.

We note, that in Ref. 12 for Xe in Ar a rate constant for energy transfer of $S=6\times10^{-8}$ cm sec^{-1} was determined, in particular from the line shape and the concentration dependence of the photoelectron emission yield in the n=2 exciton regime. This value results for 1 % Xe in Ar in an effective lifetime of 5×10^{-11} sec which is mainly determined by energy transfer. Thus, within the experimental accuracy this value is not far from the estimated limit for τ_T.

5.2 Xe in Ne

For 1 % Xe in Ne we find again an efficient energy transfer process from the excitons of the matrix to the guest atoms. This transfer process was also found in recent photoemission yield measurements[36]. The EDC's presented in Fig. 7 are evidence for this process. Both the shape and the energy of the two maxima observed are within the experimental accuracy the same for excitation energies corresponding to the n=1 and n=2 excitons. This behavior is very different from the results discussed above for Xe doped Ar and leads us to the following statements:

1. The relaxation time constant $\tau_R(n=2\rightarrow n=1)$ is small relative to the time constants for energy transfer τ_T. Thus an energy of $\approx$ 3.6 eV is dissipated before energy transfer takes place. We note that this is the difference of the excitation energies for the n=1 and n=2 states.

2. When the n=2 excitons are excited in the Ne matrix there is no indication for an additional relaxation to bound exciton states before energy transfer compared to n=1. This is contrary to the case of Ar where such a process very likely caused peak A (Fig. 4). For Ne the Au-background (subtracted in Fig. 7)

was the same for excitation into the n=2 and n=1 exciton states.

3. At the photon energy of 16 eV the Ne matrix is transparent and the absorbed photons ionize the Xe guest atoms directly. The EDC for the n=1 exciton is shifted by an amount of 0.7±0.2 eV to lower energies compared with the energy expected from eq. 1. In Fig. 7 this fact is evident by the distance to the diagonal line. This relaxation energy corresponds to the stokes shift of 0.9 eV for the strong emission band observed in luminescence[37]. As was discussed by Jortner et al.[38] this luminescence is due to the radiative decay of the free but phonon dressed excitons.

Thus the energy of the free n=1 excitons is transfered to the Xe guest atoms with the excitons in an intermediate state of phonon relaxation but without relaxation to the trapped state. The transferred energy is independent from the fact whether the n=1 or n=2 excitons of the Ne host are excited.

From the above observations the following time hierarchy, with τ_{ph} for the phonon relaxation time constant and τ_R^t the time constant for relaxation to trapped excitons is deduced.

$$\tau_R^t > \tau_D > \tau_T > \begin{cases} \tau_R(n=2\rightarrow n=1) \\ \tau_{ph} \end{cases}$$

From the oscillator strength of the n=1 excitons from Ref. 31 a life time $\tau_D \approx 10^{-9}$ sec for the radiative decay can be estimated. The rate constant $S\tau_o$ between $1 \leq S\tau_o \leq 10^{-2} ppm^{-1}$ from Ref. 37 for the energy transfer of Ne exciton energy to guest atoms gives an effective exciton life time τ which is mainly determined by energy transfer: $10^{-13} \leq \tau \leq 10^{-11}$ sec. Using this values we get:

$$\tau_R^t \geq \tau_D \approx 10^{-9} > \tau_T \approx 10^{-12} > \tau_R(n=2\rightarrow n=1)$$

A theoretical estimate of Webmann et al.[11] for $\tau_R(n=2\rightarrow n=1)$ with $\tau_R(n=2\rightarrow n=1) \approx 5\times10^{-13}$ sec is compatible with this time hierarchy.

Acknowledgements

We want to thank Dipl.-Phys. A. Harmsen, Dipl.-Phys. F.-J. Himpsel, Dipl.-Phys. D. Pudewill and Dipl.-Phys. V. Saile for help in the experiments and valuable discussions. The support of the experiments by Dr. M. Skibowski and Prof. W. Steinmann is gratefully acknowledged. The work was stimulated by the discussions with Prof. Joshua Jortner.

Table 1 Parameters for the band structure and exciton states of rare-gas solids as deduced from optical[2,31], photoemission yield[12,17,36] and photoelectron energy distribution measurements[14] togehter with results obtained in the present study (marked with an asterix). All energies are in eV. E_{Th}, threshold (binding) energies of occupied states with respect to the vacuum level; V_o, electron affinity; E_G, band gap energy; E(n=1), excitation energy and $B(n=1) = E_G - E(n=1)$, binding energy of the n=1 exciton state; B'(n=1), binding energy calculated from the Wannier model; $\Delta E_c = B' - B$, central cell correction; ΔSO, spin orbit splitting

	Ne	Ar	Xe	Xe/Ne	Xe/Ar
E_{Th}	20.3	13.9	9.8	11.2*	10.4*
V_o	1.4	0.3	0.5	1.4*	0.14*±0.2
E_G	21.69	14.2	9.3	12.6	10.54
E(n=1)	17.83	12.07	8.36	9.06	9.22
B(n=1)	3.86	2.13	0.94	3.54	1.32
B'(n=1)	5.24		1.0	5.28	2.4
ΔE_c			0.06	1.5*	1.08*
ΔSO (solid)				1.25±0.1*	1.3±0.1*
ΔSO (solid, calc. Ref. 28)			1.37		
ΔSO (gas)			1.31		

Table 2 Time hierarchy for decay processes in Xe doped Ar and Ne. The time constants used describe the following processes: τ_D, radiative decay; τ_R^t, relaxation to trapped excitons; $\tau_R(2\rightarrow1)$, relaxation of the n=1' to n=1 state, τ_T, energy transfer to Xe guest atoms; τ_{ph}, relaxation to the phonon dressed free exciton state.

Table 2a Experimental results for the time hierarchy from the EDC's

system	energy transfer	time constants
1 % Xe/Ar n=1	+	$\tau_D > \tau_R^t > \tau_T$
1 % Xe/Ar n=1'	+	$\tau_R^{(1'\rightarrow1)} > \tau_T$
1 % Xe/Ar n=2	+	$\tau_D > \tau_R(2\rightarrow1) > \tau_T \geq \tau_R^t$
1 % Xe/Ar $\hbar\omega > E_G$	-	
1 % Xe/Ne n=1	+	$\tau_D > \tau_T$
1 % Xe/Ne n=2	+	$\tau_D > \tau_T > \begin{cases} \tau_R^{(2\rightarrow1)} \\ \tau_{ph} \end{cases}$

Table 2b Time hierarchy from the EDC's together with theoretical calculations and estimates of the radiative decay time constants. All times are in sec. For references see text.

system	time constants
1 % Xe/Ar n=1	$\tau_D \approx 10^{-9} > \tau_R^t \approx 10^{-12} > \tau_T$
1 % Xe/Ar n=2	$\tau_D \approx 10^{-9} > \tau_R(2\rightarrow1') \approx 10^{-11} > \tau_T \geq \tau_R^t \approx 10^{-12}$
1 % Xe/Ne n=1	$\tau_R^t > \tau_D \approx 10^{-9} > \tau_T \approx 10^{-12}$
1 % Xe/Ne n=2	$\tau_R^t > \tau_D \approx 10^{-9} > \tau_T \approx 10^{-12} > \begin{cases} \tau_R^{(2\rightarrow1)} \approx 5\times10^{-13} \\ \tau_{ph} \end{cases}$

References

1a) J.B. Birks, Photophysics of Aromatic Molecules, Wiley, New York (1970)

b) S.P. McGlynn, T. Azumi, M. Kinoshita, Molecular Spectroscopy of the Triplet State, Prentice-Hall, Inc. Englewood Cliffs, New Jersey (1969)

c) R.S. Becker, Theory and Interpretation of Fluorescence and Phosphorescence,

d) B.R. Henry, M. Kasha, Ann. Rev.Phys.Chem. 19, 161 (1968)

e) J.B. Birks, I.H. Munro, Progress in Reaction Kinetics 4, 239 (1967)

f) J. Jortner, S.A. Rice, R.M. Hochstrasser, Advances in Photochemistry Vol. 7, eds. W.A. Noyes, J.N. Pitts, G. Hammond, Wiley, New York (1969)

2. For a recent review, see B. Sonntag, Dielectric and Optical Properties, in Rare Gas Solids, ed. by M.L. Klein and J.A. Venables, Academic Press, New York (1975)

3. J. Jortner, in Vacuum Ultraviolet Radiation Physics, eds. E.E. Koch, R. Haensel, and C. Kunz, Pergamon-Vieweg, Braunschweig (1974) p. 263

4. M. Creuzburg, Sol. State Comm. 9, 665 (1971) and references therein

5. R. Brodmann, R. Haensel, U. Hahn, U. Nielsen, and G. Zimmerer, in Vacuum Ultraviolet Padiation Physics, eds. E.E. Koch, R. Haensel, and C. Kunz, Pergamon-Vieweg, Braunschweig (1974) p. 344 and references therein

6. A. Bonnot, A.M. Bonnot, R. Coletti, J.M. Debever, and J. Hanus, Journ. de Phys. 35, C3-49 (1974)

7a) J. Jortner, L. Meyer, S.A. Rice and E.G. Wilson, J.Chem.Phys. 42, 4250 (1963)

b) N.G. Basov, V.A. Danilychev, Ya.M. Popov, and D.D. Khodkevich, JETP Lett. 12, 329 (1970)

8a) D.J. Bradley, D.R. Hull, M.H.R. Hutchinson McGeoch, Opt.Comm. 11, 335 (1974)

b) R.W. Dreyfus and S.C. Wallace, Opt.Comm. 13, 218 (1975)

9. A. Gedanken, J. Jortner, B. Raz, and A. Szöke, J.Chem.Phys. 57, 3456 (1972)

10a) M. Martin and S.A. Rice, Chem.Phys.Letters 7, 94 (1970)

b) M. Martin, J.Chem.Phys. 54, 3291 (1971)

11. I. Webmann and J. Jortner, to be published; see also Ref. 3 and Ref. 31

12. Z. Ophir, B. Raz, and J. Jortner, V. Saile, N. Schwentner, E.E. Koch, M. Skibowski, and W. Steinmann, J.Chem.Phys. 62, 650 (1975)

13. For example: P.M. Rentzepis Science 163, 239 (1970)

14. N. Schwentner, F.J. Himpsel, V. Saile, M. Skibowski, W. Steinmann, and E.E. Koch, Phys.Rev.Lett. 34, 528 (1975)

15. N. Schwentner, Thesis Universität München (1974)

16. N. Schwentner, F.J. Himpsel, E.E. Koch, V. Saile, and M. Skibowski, in Vacuum Ultraviolet Radiation Physics, eds. E.E. Koch, R. Haensel, and C. Kunz, Pergamon-Vieweg, Braunschweig (1974) p. 335

17a) N. Schwentner, M. Skibowski, and W. Steinmann, Phys.Rev. B8, 2965 (1973)

b) E.E. Koch, B. Raz, V. Saile, N. Schwentner, M. Skibowski, and W. Steinmann, Jap.J.Appl.Phys.Supl. 2, P2, 775 (1974)

18. E.E. Koch, V. Saile, N. Schwentner, and M. Skibowski, Chem.Phys.Lett. 28, 562 (1974)

19. E.E. Koch and M. Skibowski, Chem.Phys.Lett. 9, 429 (1971)

20. U. Backhaus, Diplomarbeit, Universität Hamburg 1973 (Int.Rep. DESY F41-73/11)

21. N. Schwentner, E.E. Koch, V. Saile, M. Skibowski, and A. Harmsen, in Vacuum Ultraviolet Radiation Physics, eds. E.E. Koch, R. Haensel, and C. Kunz, Pergamon-Vieweg, Braunschweig (1974) p. 792

22. F. O'Brien and K.J. Teegarden, Phys.Rev.Lett. 17, 919 (1966)

23. S.V. Pepper, J.Opt.Soc.Am. 60, 805 (1970)

24. K. Platzöder and W. Steinmann, J.Opt.Soc.Am. 58, 588 (1968)

25. A. Harmsen, E.E. Koch, V. Saile, N. Schwentner, and M. Skibowski, in Vacuum Ultraviolet Radiation Physics, eds. E.E. Koch, R. Haensel, and C. Kunz, Pergamon-Vieweg, Braunschweig (1974) p. 339

26. G. Baldini and R.S. Knox, Phys.Rev.Lett. 11, 127 (1963)

27. R.B. Cairns and J.A.R. Samson, J.Opt.Soc.Am. 56, 1568 (1966)

28. U. Rössler, phys.stat.sol. (b) 42, 345 (1970)

29. A.G. Molchanov, Kratkie soobshch. fiz 4, 9 (1972)

30. G. Baldini, Phys.Rev. 137, A508 (1965)

31. D. Pudewill, F.J. Himpsel, V. Saile, N. Schwentner, M. Skibowski, and E.E. Koch, phys.stat.sol. (b) in press

32. A. Gedanken, B. Raz, and J. Jortner, J.Chem.Phys. 58, 1178 (1973)

33. J. Hermanson, Phys.Rev. 150, 150 (1966)

34. Z. Ophir, N. Schwentner, B. Raz, M. Skibowski, and J. Jortner, J. Chem.Phys. 63, 1072 (1975)

35. A. Gedanken, B. Raz, and J. Jortner, J.Chem.Phys. 59, 5471 (1973)

36. D. Pudewill, F.J. Himpsel, V. Saile, N. Schwentner, M. Skibowski, E.E. Koch, and J. Jortner, J.Chem.Phys. (1976) in press

37. see for example: R.E. Packard, F. Reif, and C.M. Surko, Phys.Rev.Lett. 25, 4628 (1972);
I.Ya. Fugol, E.V. Sarchenko, and A.G. Belov, JETP Letters 16, 172 (1972); and Ref. 38

38. A. Gedanken, B. Raz, and J. Jortner, J.Chem.Phys. 52, 1630 (1973)

Figure Captions

Fig. 1 1a: Schematic scheme of the energy levels involved in photoelectron emission from doped solid rare gases depicted for the case Xe in Ar. The energies given are discussed in the text.

1b: Schematic scheme for various energy transfer and relaxation processes discussed in the text. Case I, energy transfer of free excitons to guest atoms; case II, relaxation of the free n=2 to the n=1 exciton state and subsequent energy transfer; case III, relaxation of the exciton states to trapped exciton states and subsequent energy transfer; case IV, relaxation of the hole in the host valence band and subsequent energy transfer, this process has also to be considered for cases I, II and III.

Fig. 2 Set up for simultaneous reflection and photoemission experiments. Synchrotron light (SR) enters the sample chamber (SC) from the monochromator (M) with concave grating (G) via the exit slit (ES). A cryostat (K) with two cryo-shields (CS) and an insulated sample substrate (I), an open electrostatic photomultiplier (D1), a gas handling system (GH) and an photoelectron energy analyser (EEA) with a channeltron as detector (CH) are incorporated into the sample chamber. Photoelectron analysis: V_o to V_5 lens voltages, V_p sample voltage, EM emitter follower, D discriminator, MCA multichannel analyser; DAC digital analog converter. Channel advance is triggert by a reference signal via lock in amplifier (LIA), analog digital converter (ADC) and a preset counter (PC). The reflectance as a function of wavelength is measured by D1. Filmthickness is determined by comparing the reflectance $R_1(t)$ at λ_1(VUV) and $R_2(t)$ at λ_2 (laser-wavelength, laser (L) via detector D2) simultaneously during evaporation time t.

Fig. 3 Right part (EDC's): Photoelectron energy distribution curves (counting rates versus kinetic energy) of 1 % Xe in Ar for a spectrum of photon energies. The film thickness was 50 Å. For normalization and subtraction of background see text. For convenience the relevant energy levels are shown in the insert.

Left part (Yield): The crosses represent the total number of emitted electrons from the EDC's. For comparison the yield of 1 % Xe in Ar (Ref. 12) of a 60 Å thick film is shown (solid line). The two sets of data were adjusted at $\hbar\omega$=11 and 11.5 eV (gold substrate). The energies of the n=1, 1'2 and 2' exciton states are marked.

Fig. 4 Photoelectron energy distribution curves (EDC's) of a 50 Å thick film of 1 % Xe in Ar, similar to Fig. 3. For A, B, and C see text.

Fig. 5 Comparison of photoelectron energy distribution curves (EDC's) of 1 % Xe in Ar (film thickness d=50 Å) with an EDC of pure Ar (film thickness d=45 Å) and an EDC of the gold substrate at a photon energy of $\hbar\omega$=12.25 eV. Note that the counting rates for the three curves are on the same scale.

Fig. 6 Constant final state (CFS) spectra for E_{kin} = 0.2±0.2 eV (counting rates at a fixed kinetic energy of the photoelectron versus the exciting photon energy) for Xe doped Ar, for pure Ar with different film thicknesses d and for the gold substrate. As a guideline the data points for Xe in Ar have been connected by a broken line (not a measured curve).

Fig. 7 Photoelectron energy distribution curves (EDC's) of a thin film of Xe doped Ne for three excitation energies. The spin-orbit splitting of the Xe guest levels and the relaxation energy before energy transfer are indicated.

Fig. 8 Comparison of luminescence spectra of pure Ar (solid curves, A,B,C are measurements from Ref. 35,5 and 6 respectively) with the EDC (hatched curve) of a Xe doped Ar film. The energy scale refers to the energy of the emitted photons. For the EDC it denotes the energy of the photoelectrons relative to the top of the Xe guest levels. The dashed vertical line marks the vacuum level, denoting the minimum energy required for ionization of the Xe impurity levels.

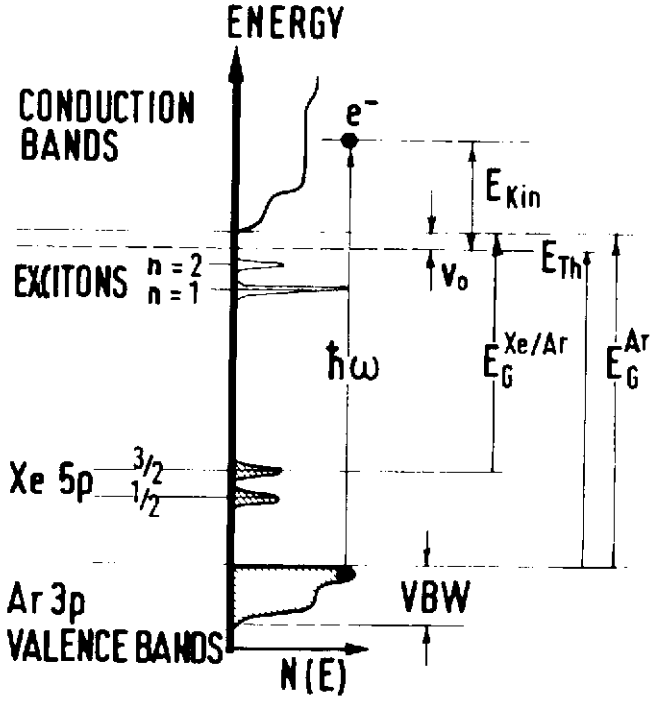

Fig. 1a

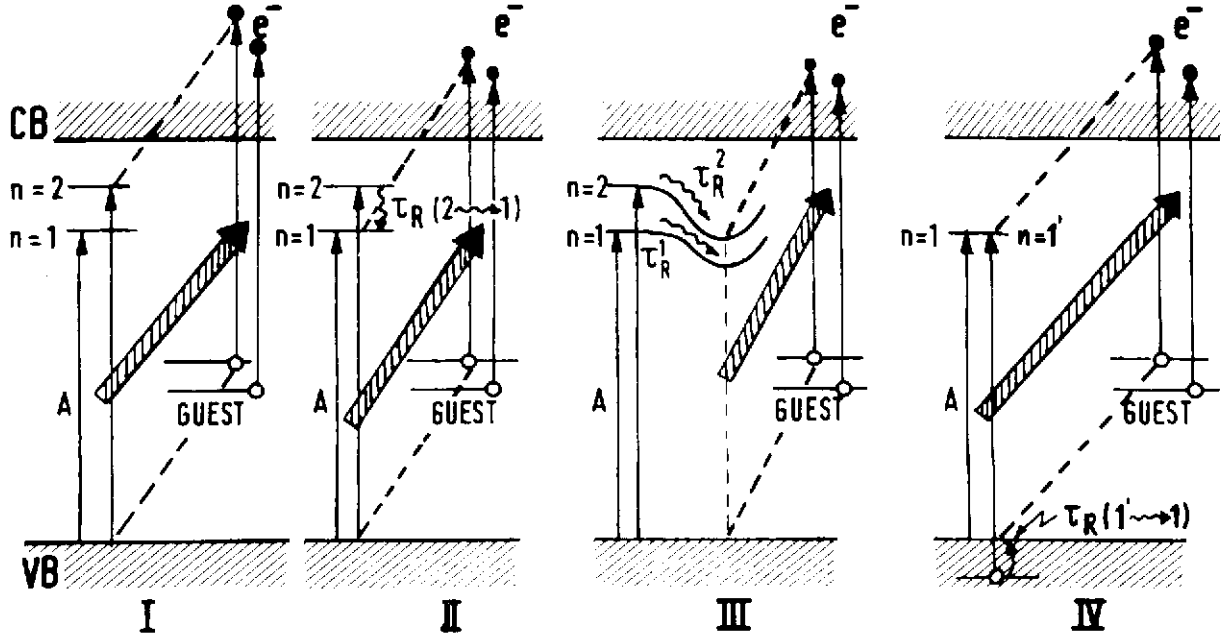

DESY

24252

Fig. 1b

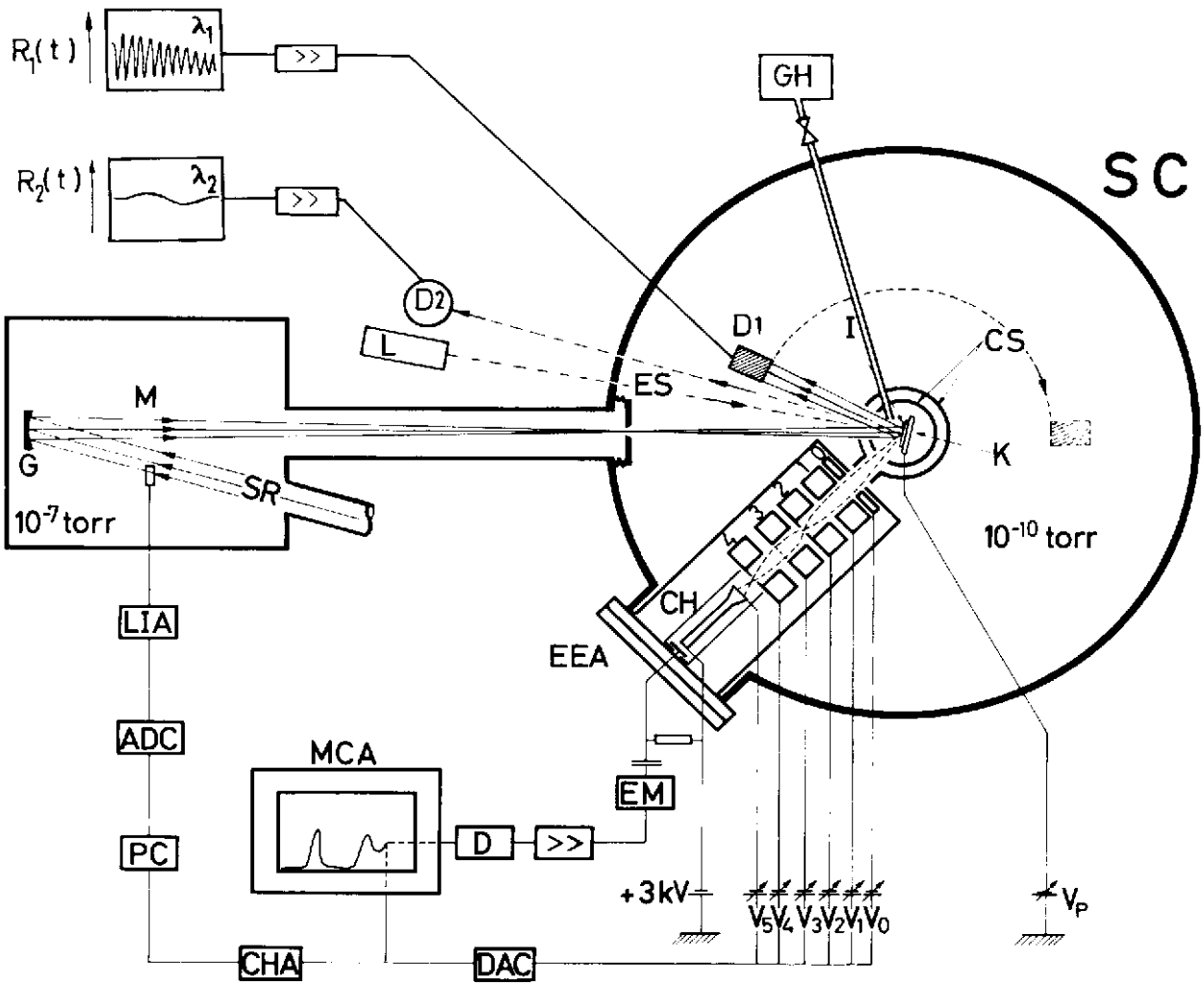
R1(t)
λ1
>>
R2(t)
λ2
>>
D2
L
GH
SC
D1
I
CS
ES
M
G
SR
10-7 torr
K
10-10 torr
CH
EEA
LIA
ADC
MCA
EM
PC
D
>>
+3kV
V5V4V3V2V1V0
VP
CHA
DAC

Fig. 2

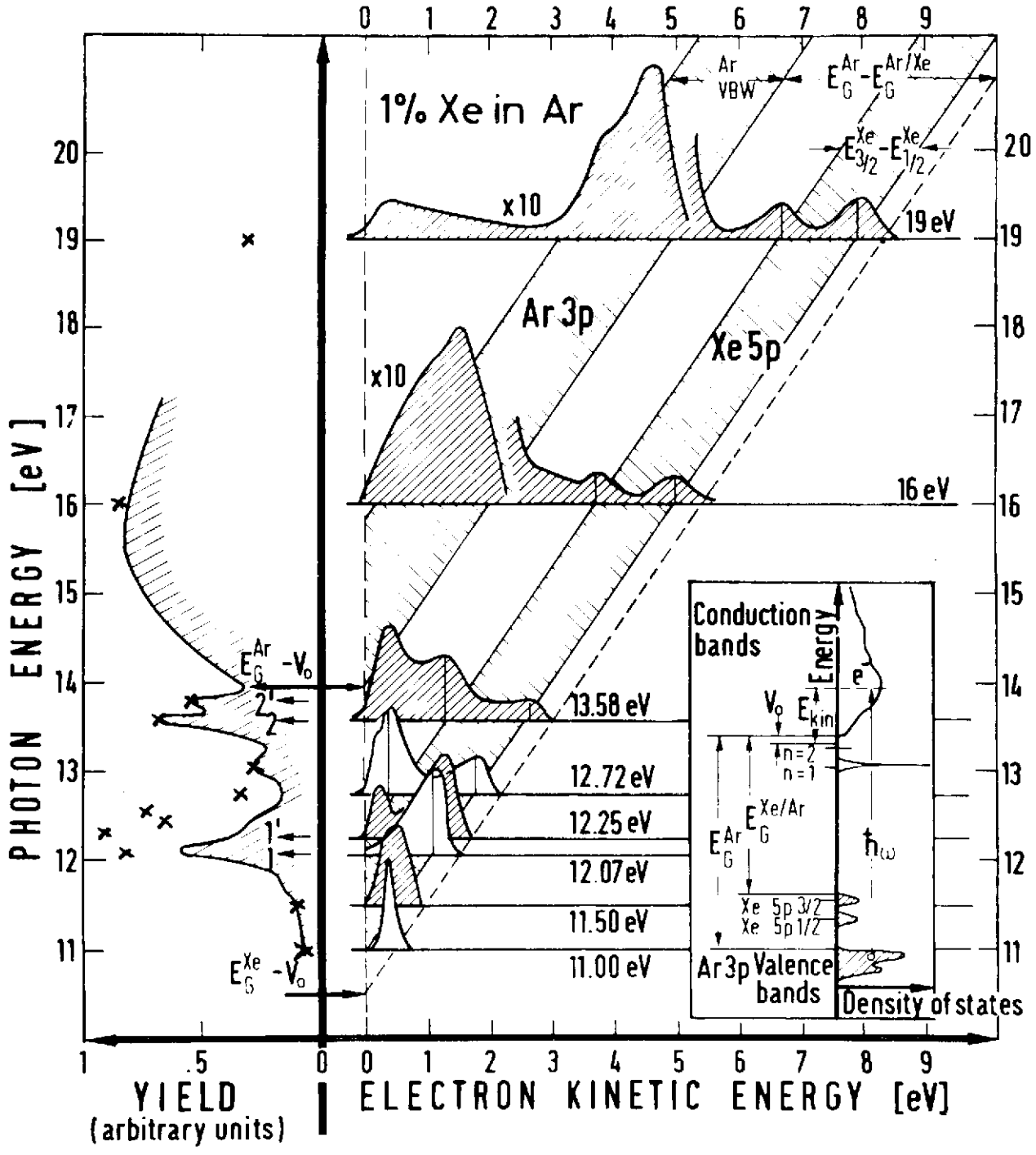
1% Xe in Ar
Ar VBW
$E_G^{Ar}-E_G^{Ar/Xe}$
$E_{3/2}^{Xe}-E_{1/2}^{Xe}$
x10
19 eV
Ar 3p
Xe 5p
x10
16 eV
13.58 eV
12.72 eV
12.25 eV
12.07 eV
11.50 eV
11.00 eV
$E_G^{Ar}-V_o$
$E_G^{Xe}-V_o$
2'
2
1'
1
Conduction bands
Energy
e
V_o E_{kin}
n=2
n=1
$E_G^{Xe/Ar}$
E_G^{Ar}
$\hbar\omega$
Xe 5p 3/2
Xe 5p 1/2
Ar 3p Valence bands
Density of states
PHOTON ENERGY [eV]
YIELD
(arbitrary units)
ELECTRON KINETIC ENERGY [eV]

Fig. 3

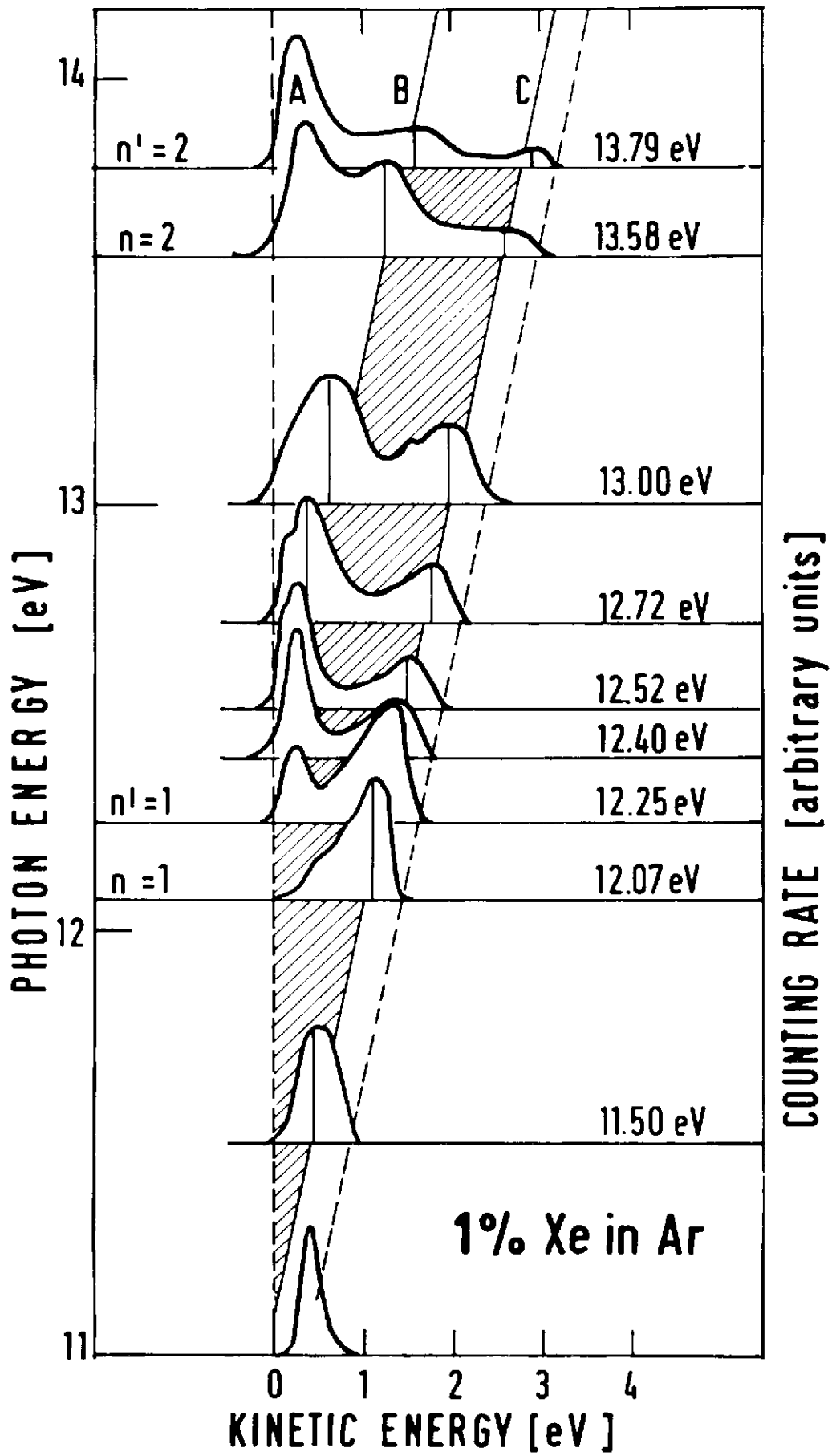
14
13
12
11
A
B
C
n' = 2
n = 2
n' = 1
n = 1
13.79 eV
13.58 eV
13.00 eV
12.72 eV
12.52 eV
12.40 eV
12.25 eV
12.07 eV
11.50 eV
1% Xe in Ar
PHOTON ENERGY [eV]
COUNTING RATE [arbitrary units]
0
1
2
3
4
KINETIC ENERGY [eV]

Fig. 4

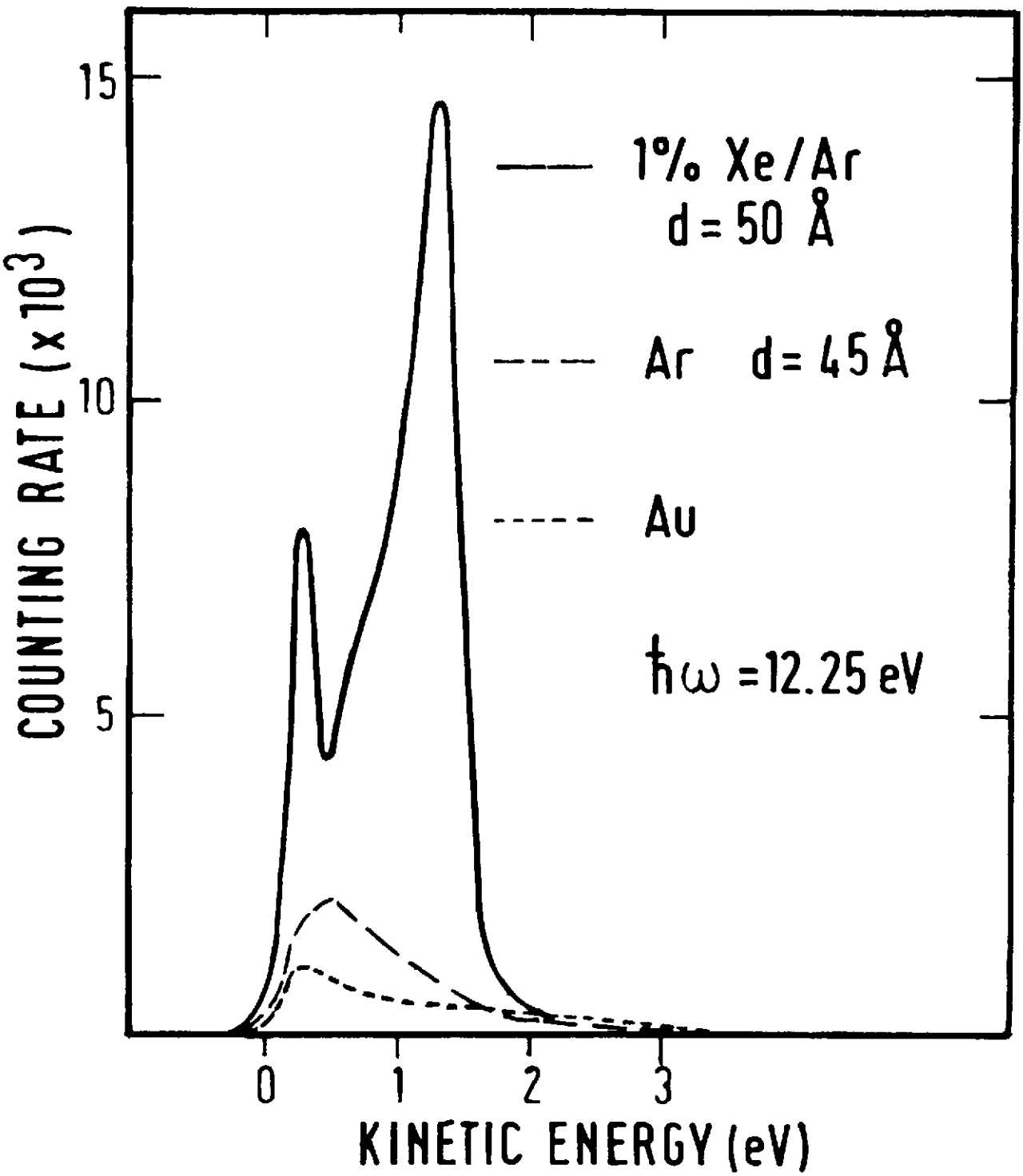
15
10
5
COUNTING RATE (x10³)
1% Xe/Ar
d = 50 Å
Ar d = 45 Å
Au
ħω = 12.25 eV
0
1
2
3
KINETIC ENERGY (eV)

Fig. 5

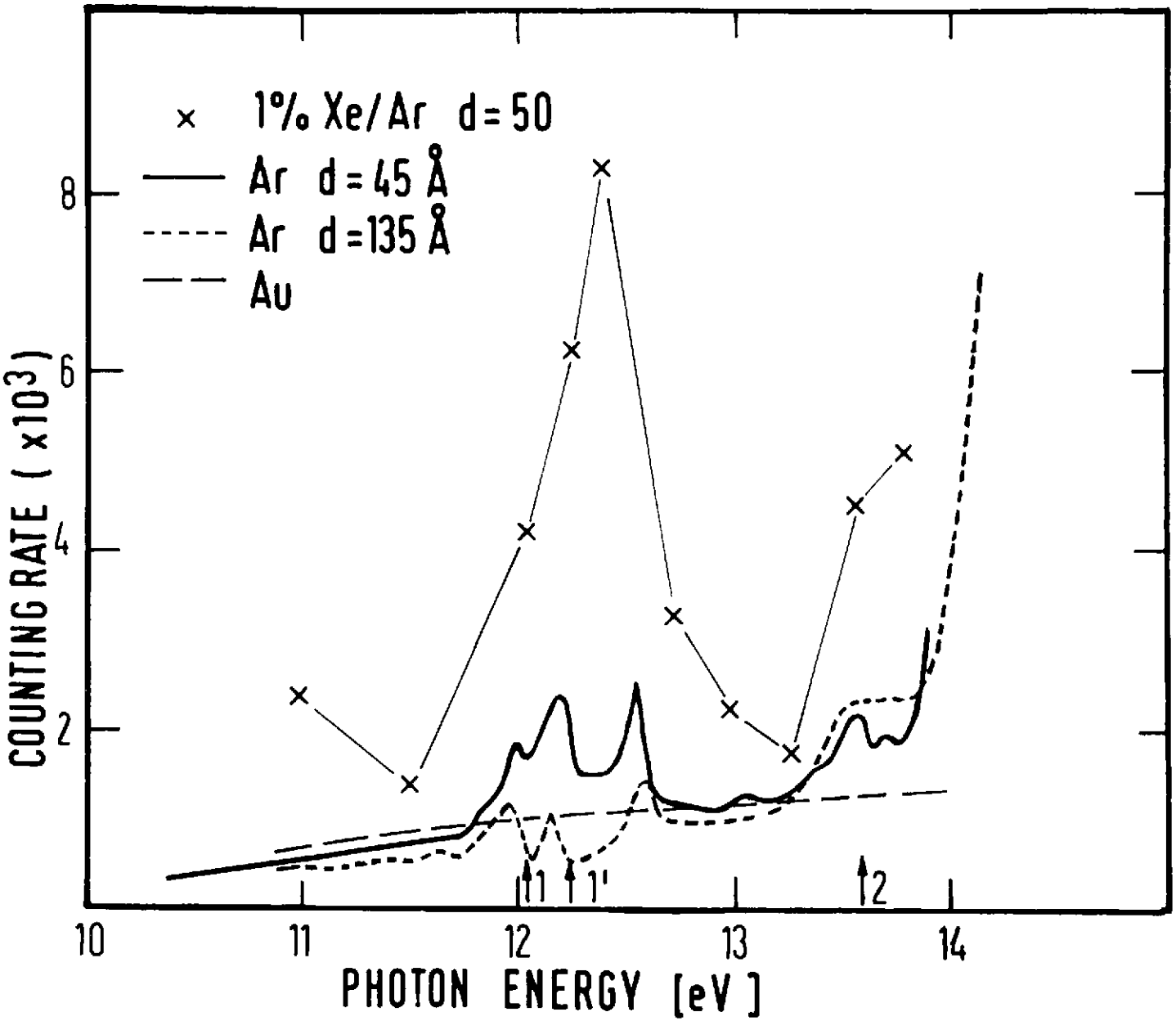

Fig. 6

DESY

24253

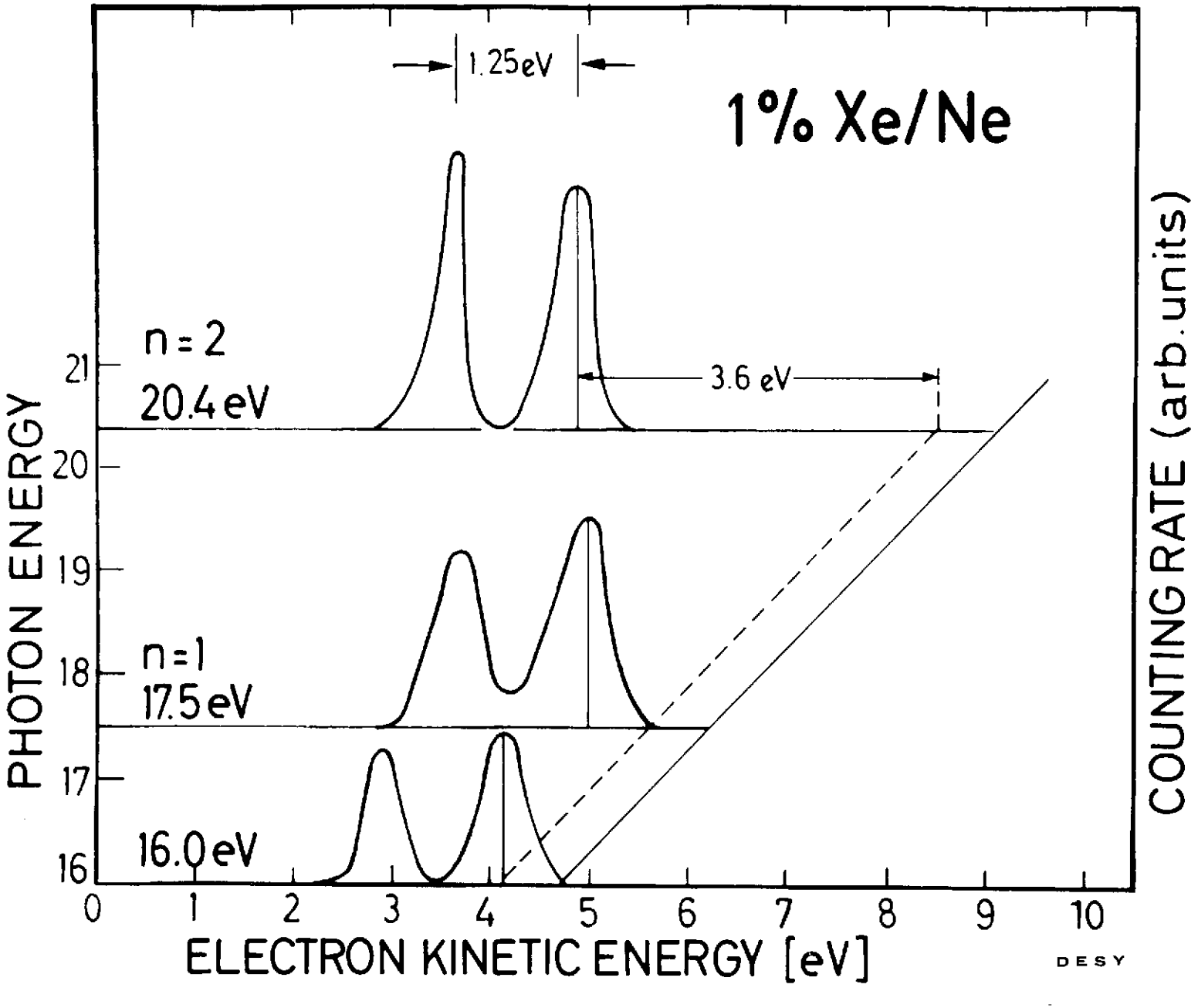
1.25eV
1% Xe/Ne
n = 2
20.4 eV
3.6 eV
n = 1
17.5 eV
16.0 eV
PHOTON ENERGY
21
20
19
18
17
16
0
1
2
3
4
5
6
7
8
9
10
ELECTRON KINETIC ENERGY [eV]
COUNTING RATE (arb. units)
DESY
24254

Fig. 7

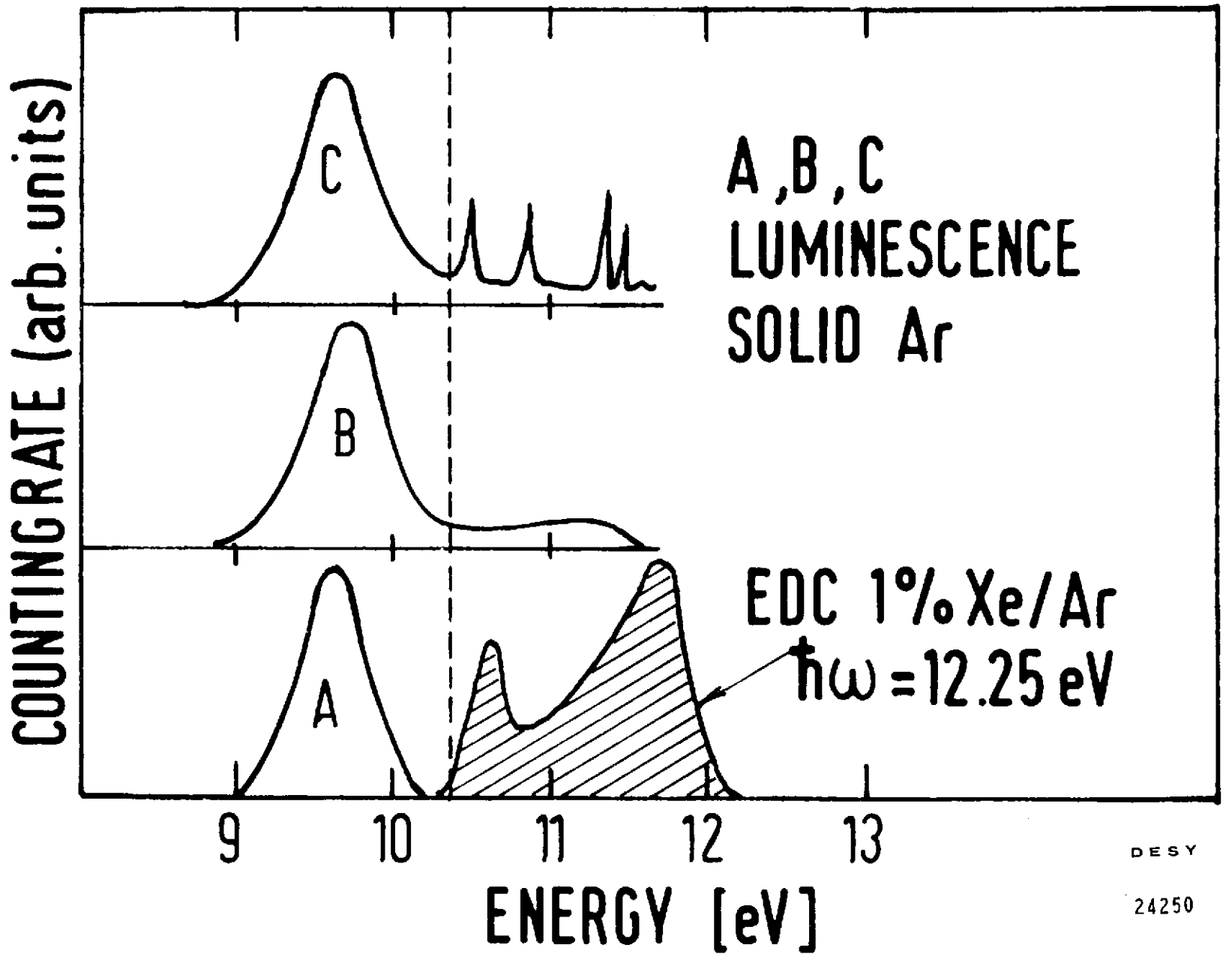
COUNTINGRATE (arb. units)
C
B
A
A, B, C
LUMINESCENCE
SOLID Ar
EDC 1% Xe/Ar
ħω = 12.25 eV
9
10
11
12
13
ENERGY [eV]
DESY
24250

Fig. 8